COMMUNICATION

Check for updates

Tuning the redox profile of the 6,6′-biazulenic platform through functionalization along its molecular axis†

Shaun R. Kelsey, [ID] [a] Georgii Griaznov, [ID] [a] Andrew D. Spaeth, [ID] [a]
Daron E. Janzen, [ID] [b] Justin T. Douglas, [ID] [c] Ward H. Thompson [ID] [a] and
Mikhail V. Barybin [ID] *[a]

The $E_{1/2}$ potential associated with reduction of the linearly-functionalized 6,6′-biazulenic scaffold is accurately correlated to the combined σ_p Hammett parameters of the substituents over >600 mV range. X-ray crystallographic analysis of the 2,2′-dichloro-substituted derivative revealed unexpectedly short C–Cl bond distances, along with other metric changes, suggesting a non-trivial cycloheptafulvalene-like structural contribution.

Originally isolated from plant essential oils in the nineteenth century, azulenic compounds continue to fascinate scientists to this day. The correct structure of the polar azulenic scaffold, $C_{10}H_8$, ($\mu \approx 1.1$ Debye[1]) that features fused five- and seven-membered sp²-carbon rings was first recognized by Pfau and Plattner in 1936.[2] The X-ray crystallographic confirmation of azulene's molecular structure was reported 20 years later.[3,4] Azulenic building blocks are attractive for developing π-functional molecules and materials.[5–7] Among the three possible linear biazulenes, 6,6′-biazulene has recently been emerging as a particularly effective oligoazulenic π-linker in the design of molecular electron reservoirs,[8] on-chip microsupercapacitors,[9] quasi-molecular rectifiers,[10] organic and organometallic self-assembled monolayer (SAM) films,[8,11] and organic field-effect transistors.[12] Since the synthesis of 6,6′-biazulene in 1980,[13] access to its derivatives, especially those functionalized along its molecular axis, has been quite limited.[11,14,15]

[a] *Department of Chemistry, University of Kansas, Lawrence, KS 66045, USA.*
  E-mail: mbarybin@ku.edu

[b] *Department of Chemistry and Biochemistry, St. Catherine University, St. Paul,
  MN 55105, USA*

[c] *NMR Laboratory, Molecular Structures Group, University of Kansas, Lawrence,
  KS 66047, USA*

† Electronic supplementary information (ESI) available: Experimental procedures, spectroscopic and analytical data, details of the electrochemical, X-ray crystallographic and DFT studies. CCDC 2300779. For ESI and crystallographic data in CIF or other electronic format see DOI: https://doi.org/10.1039/d4cc00656a

Given that azulene's highest occupied and lowest unoccupied molecular orbitals (HOMO/LUMO) have complementary orbital density distributions, their energies can be varied independently, to a first approximation.[16–18] This is accomplished by considering the position of attachment of a substituent to the azulenic core, as well as its electron withdrawing/donating ability.[19] In this communication, we envisioned a similar approach for tailoring the energetics of the frontier molecular orbitals of the linear 6,6′-biazulenic framework. Indeed, Fig. 1 illustrates the orbital density complementarity between the HOMO and LUMO of 6,6′-biazulene.

Herein, we demonstrate that the redox potential ($E_{1/2}$) of the 6,6′-biazulenic scaffold is accurately predictable based on the Hammett σ_p parameters[20] of the substituents X and X′ incorporated along its molecular axis (Fig. 2). To the best of our knowledge, this is the first study unveiling such quantitative redox correlations in the context of azulenic π-systems. In addition, we discuss how dichloro substitution exerts unexpected structural permutations within compound **3a** (X = X′ = Cl) in the solid state.

To facilitate synthetic accessibility of 2,2′-functionalized 6,6′-biazulenes, we selected the 1,1′,3,3′-tetraethoxycarbonyl-6,6′-biazulene (**1**) as the "parent" platform. Rather than employing a toxic organotin reagent to assemble **1** *via* Stille cross-coupling,[21] our synthesis of this compound involved simple deamination of the biazulenic derivative **2a** (Scheme 1). On the other hand, subjecting **2a** to Sandmeyer chlorination afforded dark purple, nearly black, crystalline
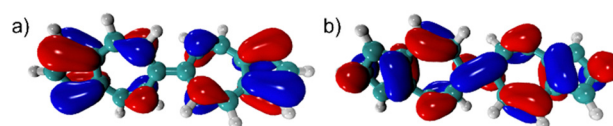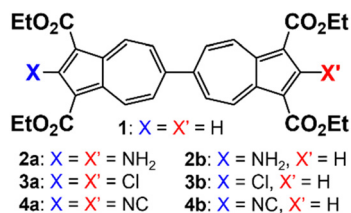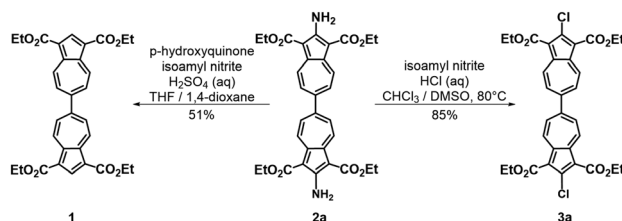

Fig. 1 Highest occupied (a) and lowest unoccupied (b) molecular orbitals (HOMO and LUMO) of 6,6′-biazulene (B3LYP functional and cc-pVDZ basis set).

Fig. 2 2,2′-Functionalized 6,6′-biazulenes considered in this work.
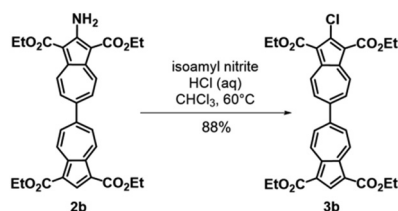

Scheme 1 Syntheses of 1,1′,3,3′-tetraethoxycarbonyl-6,6′-biazulene (**1**) and 2,2′-dichloro-1,1′,3,3′-tetraethoxycarbonyl-6,6′-biazulene (**3a**).

2,2′-dichloro-1,1′,3,3′-tetraethoxycarbonyl-6,6′-biazulene (**3a**) in an 85% yield (Scheme 1). Thus, **3a** can be prepared from 2-amino-6-bromo-1,3-diethoxycarbonylazulene[22] in two steps with an overall yield of *ca.* 80% (Scheme S1, ESI†).[14] In addition to **3a**, we synthesized its unsymmetric congener, 2-chloro-1,1′,3,3′-tetraethoxycarbonyl-6,6′-biazulene (**3b**), *via* Sandmeyer chlorination of our recently reported 2-amino-1,1′,3,3′-tetraethoxycarbonyl-6,6′-biazulene (**2b**) (Scheme 2).[8] Both **3a** and **3b** constitute versatile precursors to a variety of 2-, and 2,2′-functionalized 6,6′-biazulenes.

Given that unsymmetrically functionalized **3b** is a structural hybrid of centrosymmetric **1** and **3a**, it is reasonable that its ^{1}H NMR spectrum (Fig. S7, ESI†) appears as a superposition of the ^{1}H patterns observed for the latter compounds (Fig. S1 and S2, ESI†).

We assigned all resonances in the ^{13}C NMR spectrum of **3a** *via* synergistic consideration of its HSQC, HMBC, and 1,1-ADEQUATE[23–26] 2-D maps (Fig. S3–S6, ESI†). Notably, this is the only unambiguously assigned ^{13}C NMR profile of any 6,6′-biazulene reported in the literature to date.

Our TD-DFT calculations (Table S4, ESI†) corroborate that the lowest energy broad band centered around 500 nm in the electronic absorption spectrum of **3a** (Fig. 3a) corresponds to the HOMO → LUMO and HOMO−1 → LUMO transitions. The broad nature of this band can be attributed, in part, to the range of accessible microstates pertaining to the

Scheme 2 Synthesis of 2-chloro-1,1′,3,3′-tetraethoxycarbonyl-6,6′-biazulene (**3b**).
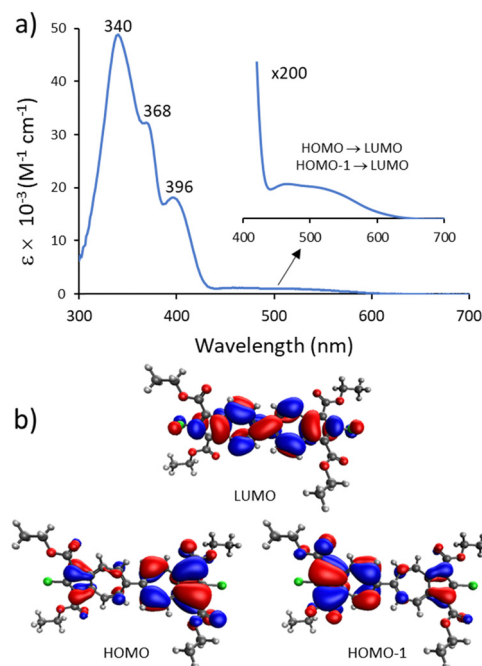

Fig. 3 (a) Electronic absorbance spectrum of **3a** in CH_2Cl_2 at 22 °C. (b) TD-DFT calculated molecular orbitals of **3a** involved in the $S_0 \rightarrow S_1$ transition.

azulene–azulene interplanar angle within **3a** in CH_2Cl_2 solution.[11] While the LUMO of **3a** involves the entire biazulenic core, **3a**'s nearly degenerate HOMO and HOMO−1 are each primarily localized on one of the azulenic units (Fig. 3b).

We have recently shown that 2,2′-functionalized 6,6′-biazulenes undergo reversible one-step, 2e[−] reduction in CH_2Cl_2/[n]-$Bu_4N^+PF_6^−$ solutions under the potential inversion regime[27] regardless of whether they feature symmetric or asymmetric substitution along their molecular axis.[8] After recognizing a qualitative relationship between the $E_{1/2}$ values associated with the 2e[−] reduction of the 6,6′-biazulenic core and the electron donating/withdrawing characteristics of the 2,2′-substituents, we set out to identify a quantitative approach for tuning the 6,6′-biazulenic redox profile (Fig. S13–S16, ESI†). Remarkably, plotting the half-wave redox potential ($E_{1/2}$) against the combined σ_p Hammett parameters[20] of the substituents X and X′ for the seven 6,6′-biazulenic derivatives listed in Fig. 2 revealed a nearly perfect linear correlation over >600 mV range (Fig. 4 and Table S5, ESI†). While attempts to correlate molecular redox potentials with the Hammett parameters of functional groups have been reported in the past for benzenoid organic/organometallic and ferrocene-based compounds,[28–31] this is the first example of invoking such a relationship for a cohort of azulenic derivatives. Notably, a similar trend ($E_{p,c}$ *vs.* σ_p) holds for the family of 2-substituted 1,3-diethoxycarbonyl azulenes shown in Fig. 5 and Table S6 (ESI†). However, the 1e[−] reduction of the latter compounds is invariably irreversible (Fig. S17–S20, ESI†).[11] Coupling any pair of 2-substituted azulenes to form the corresponding 6,6′-biazulene leads to full reversibility of the reduction, with the biazulenic $E_{p,c}$
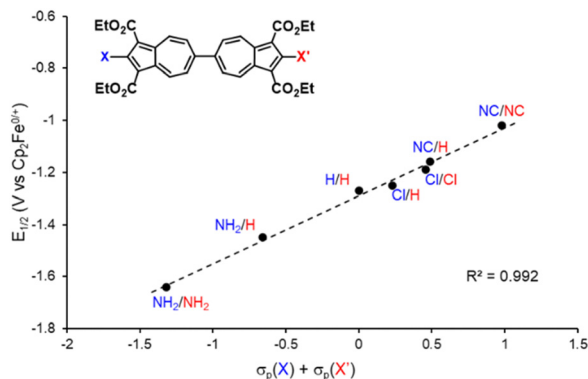
Fig. 4 A plot of the 2e⁻ reduction potential ($E_{1/2}$) for 2,2′-functionalized 6,6′-biazulenes vs. the combined σ_p Hammett parameters of the substituents X and X′.
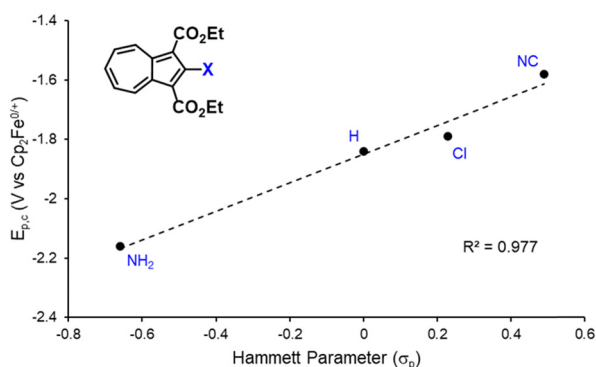

Fig. 5 A plot of the reduction potential ($E_{p,c}$) for 2-functionalized 1,3-diethoxycarbonylazulenes vs. the σ_p Hammett parameter of the substituent X.

being 0.51 ± 0.04 V more positive compared to the average $E_{p,c}$ of the monoazulenes (Tables S5 and S6, ESI†). This is a consequence of the substantially greater resonance stabilization energy of the 6,6′-biazulenic framework.

The molecular structure of **3a** is illustrated in Fig. 6. The two chemically identical, but crystallographically unique C–Cl bonds, C2–Cl1 and C2′–Cl2, within **3a** have the lengths of 1.674(2) Å and 1.682(2) Å, respectively. The longer C–Cl bond
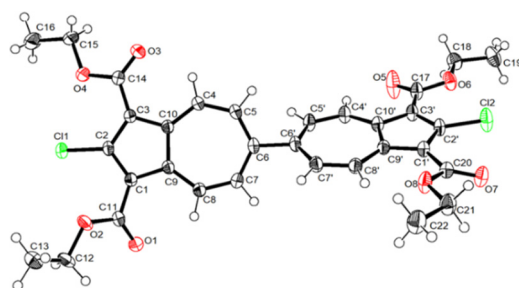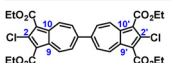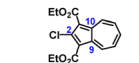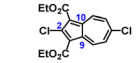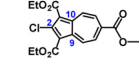

Fig. 6 Molecular structure of **3a** (50% thermal ellipsoids). Selected interatomic distances (Å) and dihedral angle (deg): C2–Cl1 1.674(2), C2′–Cl2 1.682(2), C6–C6′ 1.478(2), C9–C10 1.437(2), C9′–C10′ 1.440(3), O2⋯Cl1 2.918(2), O4⋯Cl1 2.834(1), O6⋯Cl2 2.816(2), O7⋯Cl2 2.876(2), C5–C6–C6′–C5′ 48.1(2).

Table 1 Comparison of C(2)–Cl and C(9)–C(10) bond distances in X-ray structurally characterized 2-chloroazulenic derivatives

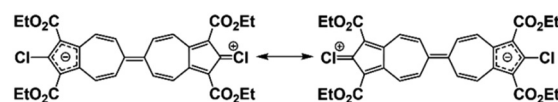| Compound	$d(C^2–Cl)$ Å	$d(C^9–C^{10})$ Å	CCDC identifier
	1.674(2) 1.682(2)	1.437(2) 1.440(3)	This work
	1.712(2)	1.471(2)	HOMRAE
	1.714(4)	1.470(6)	XIGPOU
	1.709(2)	1.470(3)	AYIDIX

Fig. 7 Minor zwitterionic resonance forms of **3a**.

belongs to the half of the molecule featuring the shortest Cl⋯O contact (Cl2⋯O6) of 2.816 Å. Both C–Cl bonds in **3a** are significantly shorter than any C–Cl bond in all structurally characterized chloroazulenes featuring Cl-substitution at the five-membered ring of the azulenic scaffold (Fig. S22 and Table S14, ESI†). In particular, the C–Cl bonds in **3a** are statistically shorter, per the 3-σ criterion,[32] than those in the X-ray structures of the other three 2-chloroazulenes known to date (Table 1).[33–35]

The C–Cl bond contractions in **3a** may be rationalized by invoking the minor heptafulvalene-like zwitterionic resonance forms depicted in Fig. 7, which show C=Cl double-bond character. This argument mirrors the crystallographic analysis of the chlorodiphenylmethylium cation by Laub et al.[36] The short C–Cl bond distance of 1.668(8) Å within this carbocation, which is statistically indistinguishable from those in **3a**, was attributed to chlorine back-donation exerting partial double-bond C=Cl⁺ character (Fig. S23, ESI†).[36] Unusually short C–Cl bonds, including various C–Cl multiple bonding scenarios, continue to attract both experimental and theoretical interest.[37–39]

The C6–C6′ bond distance of 1.478(2) Å within **3a** is markedly shorter than those in all other crystallographically characterized 6,6′-biazulenes (Table 2).[8,11,12,40] In addition, as summarized in Table 2, the C–C bonds at the fusion of the five- and seven-membered rings in **3a** are substantially contracted as well. Both of these observations are consistent with a nontrivial heptafulvalene-like contribution to the structure of the biazulenic scaffold of **3a**.[41] Moreover, the azulene–azulene interplanar angles in dichloro **3a** and diisocyano **4a**, which share the same 1,1′,3,3′-tetraethoxycarbonyl-6,6′-biazulenic core, are 48.1° and 66.9°,[11] respectively, although such comparison should be viewed cum grano salis as this torsion parameter is undoubtedly sensitive to crystal packing.

In summary, we demonstrated that the redox profile of the 6,6′-biazulenic scaffold functionalized along its molecular axis is quantitatively tuneable within a wide window of potentials.

Table 2 Comparison of C(6)−C(6′) and C(9)−C(10) bond distances in X-ray structurally characterized 6,6′-biazulenes

Compound	$d(C^6-C^{6'})$, Å	$d(C^9-C^{10})$ Å	CCDC identifier
	1.478(2)	1.437(2) / 1.440(3)	This work
	1.498(2)	1.485(2) / 1.488(2)	NAZROZ
	1.512(4)	1.475(3)	OSIGED
	1.497(3) / 1.499(3)	1.465(3)–1.476(3)	HITRIP[a]

[a] Two crystallographically independent molecules in the asymmetric unit.

This was accomplished by considering, for the first time in the context of azulenic systems, the well documented σ_p Hammett parameters[20] reflecting the net electronic influence of the substituents. We anticipate that the facile access to the crystallographically unusual dichloro derivative **3a** offers not only new opportunities to engage the 6,6′ architecture as an attractive molecular template in the realm of organic charge transfer and/or conductive materials, but also to explore unorthodox approaches for pursuing C–Cl multiple bonding.

Conflicts of interest

There are no conflicts to declare.

Notes and references

1 A. G. Anderson and B. M. Steckler, *J. Am. Chem. Soc.*, 1959, **81**, 4941–4946.
2 A. St. Pfau and P. A. Plattner, *Helv. Chim. Acta*, 1936, **19**, 858–879.
3 J. M. Robertson and H. M. M. Shearer, *Nature*, 1956, **177**, 885.
4 J. M. Robertson, H. M. M. Shearer, G. A. Sim and D. G. Watson, *Nature*, 1958, 177–178.
5 H. Katagiri, in *Advances in Organic Crystal Chemistry*, ed. H. Uekusa and M. Sakamoto, Wiley, 2020, pp. 341–358.
6 J. Huang, S. Huang, Y. Zhao, B. Feng, K. Jiang, S. Sun, C. Ke, E. Kymakis and X. Zhuang, *Small Methods*, 2020, **4**, 2000628.
7 H. Xin, B. Hou and X. Gao, *Acc. Chem. Res.*, 2021, **54**, 1737–1753.
8 P. T. Connelly, J. C. Applegate, D. A. Maldonado, M. K. Okeowo, W. C. Henke, A. G. Oliver, C. L. Berrie and M. V. Barybin, *Dalton Trans.*, 2023, **52**, 11419–11426.
9 C. Yang, K. S. Schellhammer, F. Ortmann, S. Sun, R. Dong, M. Karakus, Z. Mics, M. Löffler, F. Zhang, X. Zhuang, E. Cánovas, G. Cuniberti, M. Bonn and X. Feng, *Angew. Chem., Int. Ed.*, 2017, **56**, 3920–3924.
10 S. Sun, X. Zhuang, L. Wang, B. Zhang, J. Ding, F. Zhang and Y. Chen, *J. Mater. Chem. C*, 2017, **5**, 2223–2229.
11 T. R. Maher, A. D. Spaeth, B. M. Neal, C. L. Berrie, W. H. Thompson, V. W. Day and M. V. Barybin, *J. Am. Chem. Soc.*, 2010, **132**, 15924–15926.
12 Y. Shibuya, K. Aonuma, T. Kimura, T. Kaneko, W. Fujiwara, Y. Yamaguchi, D. Kumaki, S. Tokito and H. Katagiri, *J. Phys. Chem. C*, 2020, **124**, 4738–4746.
13 M. Hanke and C. Jutz, *Synthesis*, 1980, 31–32, DOI: 10.1055/s-1980-28911.
14 An alternative synthesis of **3a** from 2-amino-6-bromo-1,3-diethoxycarbonylazulene, albeit in a three-step sequence with an overall *ca.* 45% yield, has been recently reported: B. Hou, Z. Zhou, C. Yu, X. S. Xue, J. Zhang, X. Yang, J. Li, C. Ge, J. Wang and X. Gao, *ACS Macro Lett.*, 2022, **11**, 680–686.
15 Y. Yamaguchi, M. Takubo, K. Ogawa, K. Nakayama, T. Koganezawa and H. Katagiri, *J. Am. Chem. Soc.*, 2016, **138**, 11335–11343.
16 R. S. H. Liu and A. E. Asato, *J. Photochem. Photobiol., C*, 2003, **4**, 179–194.
17 R. S. H. Liu, *J. Chem. Ed.*, 2002, **79**, 183–185.
18 R. P. Steer, *J. Photochem. Photobiol., C*, 2019, **40**, 68–80.
19 R. E. Robinson, T. C. Holovics, S. F. Deplazes, D. R. Powell, G. H. Lushington, W. H. Thompson and M. V. Barybin, *Organometallics*, 2005, **24**, 2386–2397.
20 R. W. Taft, A. Leo and C. Hansch, *Chem. Rev.*, 1991, **91**, 165–195.
21 S. Ito, T. Okujima and N. Morita, *J. Chem. Soc., Perkin Trans. 1*, 2002, 1896–1905.
22 T. C. Holovics, R. E. Robinson, E. C. Weintrob, M. Toriyama, G. H. Lushington and M. V. Barybin, *J. Am. Chem. Soc.*, 2006, **128**, 2300–2309.
23 G. E. Martin, *Annual Reports on NMR Spectroscopy*, Elsevier, 2011, ch. 5, vol. 74, pp. 215–291.
24 B. D. Hilton, K. A. Blinov and G. E. Martin, *J. Nat. Prod.*, 2011, **74**, 2400–2407.
25 M. M. Senior, R. T. Williamson and G. E. Martin, *J. Nat. Prod.*, 2013, **76**, 2088–2093.
26 A. V. Buevich, R. T. Williamson and G. E. Martin, *J. Nat. Prod.*, 2014, **77**, 1942–1947.
27 D. H. Evans, *Chem. Rev.*, 2008, **108**, 2113–2144.
28 L. Wang, Z. L. Xie, B. T. Phelan, V. M. Lynch, L. X. Chen and K. L. Mulfort, *Inorg. Chem.*, 2023, **62**, 14368–14376.
29 J. C. Dickenson, M. E. Haley, J. T. Hyde, Z. M. Reid, T. J. Tarring, D. A. Iovan and D. P. Harrison, *Inorg. Chem.*, 2021, **60**, 9956–9969.
30 W. C. Henke, D. Lionetti, W. N. G. Moore, J. A. Hopkins, V. W. Day and J. D. Blakemore, *ChemSusChem*, 2017, **10**, 4589.
31 N. Vo, N. L. Haworth, A. M. Bond and L. L. Martin, *ChemElectroChem*, 2018, **5**, 1–14.
32 F. Pukelsheim, *Am. Stat.*, 1994, **48**, 88–91.
33 S. Förster, W. Seichter, R. Kuhnert and E. Weber, *J. Mol. Struc.*, 2014, **1075**, 63–70.
34 K. J. Scheetz, A. D. Spaeth, A. S. Vorushilov, D. R. Powell, V. W. Day and M. V. Barybin, *Chem. Sci.*, 2013, **4**, 4267–4272.
35 B. B. Ling, *CSD Commun.*, 2016, CCDC 888557, DOI: 10.5517/ccdc.csd.ccytm4h.
36 T. Laube, E. Bannwart and S. Hollenstein, *J. Am. Chem. Soc.*, 1993, **115**, 1731–1733.
37 F. Fantuzzi, B. Rudek, W. Wolff and M. A. C. Nascimento, *J. Am. Chem. Soc.*, 2018, **140**, 4288–4292.
38 R. Kalescky, E. Kraka and D. Cremer, *Int. J. Quantum Chem.*, 2014, **114**, 1060–1072.
39 M. Göbel, B. H. Tchitchanov, J. S. Murray, P. Politzer and T. M. Klapotke, *Nat. Chem.*, 2009, **1**, 229–235.
40 Not included in Table 2 is the structure of 2,2′-dibromo-1,1′-dibutyl-6,6′-biazulene that is searchable in CCDC (NAPSUW) but suffers from low precision {*e.g.*, d(C6–C6′) = 1.50(2) Å}, unacceptable data/refinement quality (*R*-factor = 11.7%), and lack of a published synthesis: B. Hou, *CSD Commun.*, 2021, CCDC 2127392.
41 R. Thomas and P. Coppens, *Acta Crystallogr., Sect. B: Struct. Crystallogr. Cryst. Chem.*, 1972, **28**, 1800–1806.